Octamethyl-1,1′-diphosphachromocene: Its Spin Distribution and Oxidation

Robert Feher,[1a] Frank H. Köhler,*[,1b] François Nief,*[,1b] Louis Ricard,[1b] and Stefan Rossmayer[1a]

Anorganisch-chemisches Institut, Technische Universität München, D-85747 Garching, Germany, and Ecole Polytechnique, CNRS URA 1499, F-91128 Palaiseau, France

Received July 2, 1997[⊗]

Octamethyl-1,1′-diphosphachromocene ($(Tmp)_2Cr$) was prepared from (Tmp)K and chromium dichloride in 81% yield. According to X-ray analysis, it has a distorted sandwich structure with the P atoms being bent away from chromium. Large ^1H, ^{13}C, and ^{31}P NMR shifts established the similarity to chromocenes ($S = 1$) and negative spin on the ligands. The signal splitting and temperature-dependent ^1H NMR data revealed that, on the ligand, the spin sits predominantly at the phosphorus and two carbon atoms. In the cyclic voltammetry, two oxidation steps and one reduction were visible. After chemical oxidation, $[(Tmp)_2Cr]^+[B(C_6H_5)_4]^-$ was isolated in 65% yield. Its EPR spectrum is in accord with a $S = {}^3/_2$ species. The ^1H NMR spectrum resembled those of chromocenium ions. Its analysis and that of the temperature-dependent ^1H NMR spectra indicated a rather uniform spin distribution within the ligands. It was concluded that, in any case, the phosphorus may release spin to neighboring molecules.

Introduction

Phospholyl ligands are susceptible of π bonding to transition metals very much like cyclopentadienyl (Cp), thus yielding phosphametallocenes.[2] As for the parent metallocenes, they have never ceased to attract attention. In particular, paramagnetic metallocenes have experienced a remarkable renaissance, because they have led to novel molecule-based magnetic materials of the type $[metallocene]^+[TCNE]^-$.[3] These materials undergo a transition from the desirable ferromagnetic to paramagnetic behavior below 10 K. In order to raise this temperature, improving the interaction between the building blocks has been attempted, for instance, by varying the metal M and the radical anion.[3] Another possibility to tune these materials consists in changing the ligands of the metallocene. We have outlined in detail previously[4] how the number and type of the substituents at Cp would localize the unpaired electron spin density within the ligand at certain carbon atoms, which in turn could improve the magnetic interaction. A pronounced effect is to be expected from replacing a CH fragment of Cp by a heteroelement, and a promising candidate in this regard is the phospholyl ligand. Since compounds like $[metallocene]^+[TCNE]^-$ form stacks that are parallel, the interaction *within* the stack might be improved by changing the spin distribution within the π ligand upon replacing Cp^* by a phospholyl ligand. In addition, the phospholyl may open a new pathway of magnetic exchange *between* the stacks when the donor capability of phosphorus leads to an interaction with the metal of the sandwich of a neighboring stack. We have embarked on tuning the paramagnetic sandwich by synthesizing octamethyl-1,1′-diphosphachromocene, ($(Tmp)_2Cr$[5]). Subsequently, we studied its oxidation to $[Tmp_2Cr]^+$, the building block necessary for stacks, and the spin distribution within both species.

Results and Discussion

The existence of phosphachromocenes was established by Nixon's pioneering synthesis of $(t\text{-}Bu_2C_2P_3)_2Cr$.[6a] Since the yield was lower than 1%[6b] we chose the more readily accessible Tmp^- ligand.[7] It has the additional advantage of being very similar to the parent phospholyl $PC_4H_4^-$ so that theoretical studies[8] could be used as guidelines.

The neutral octamethyl-1,1′-diphosphachromocene, $(Tmp)_2Cr$, was synthesized in 81% yield from Tmp^- as red air-sensitive crystals, as illustrated in Scheme 1. The structure, which was determined by X-ray analysis, is similar to that of 1,1′-diphosphaferrocenes[9] (Figure 1). The ligands are fully staggered, which results in the molecular symmetry C_{2h}. The phosphorus atom is bent away from chromium in such a way that the planes C2, P1, C5 and C2, C3, C4, C5 include an angle of 4.1°, and the distance of chromium from the plane C2, C3, C4, C5 is 1.76 Å. This distance is longer than that found for similar iron derivatives[9] by 0.13 Å, a value that was

[⊗] Abstract published in *Advance ACS Abstracts,* September 15, 1997.

(1) (a) Technische Universität München. (b) Ecole Polytechnique.

(2) Mathey, R. *New J. Chem.* **1987**, *11*, 585−593. Nixon, J. F. *Chem. Soc. Rev.* **1995**, 319−328. For bent phosphametallocenes, see: Nief, F.; Ricard, L.; Mathey, F. *Organometallics* **1989**, *8*, 1473−1477. Baudry, D.; Ephritikhine, M.; Nief, F.; Ricard, L.; Mathey, F. *Angew. Chem., Int. Ed. Engl.* **1990**, *29*, 1485−1486. Gosink, H.-J.; Nief, F.; Ricard, L.; Mathey, F. *Inorg. Chem.* **1995**, *34*, 1306−1307.

(3) Miller, J. S.; Epstein, A. J. *Angew. Chem., Int. Ed. Engl.* **1994**, *33*, 385−415. Gatteschi, D. *Adv. Mater.* **1994**, *6*, 635−645.

(4) Blümel, J.; Hebendanz, N.; Hudeczek, P.; Köhler, F. H.; Strauss, W. *J. Am. Chem. Soc.* **1992**, *114*, 4223−4230.

(5) Acronym derived from bis(η^5-tetra*m*ethyl*p*hospholyl)chromium.

(6) (a) Bartsch, R.; Hitchcock, P. B.; Nixon, J. F. *J. Organomet. Chem.* **1988**, *356*, C1−C4. (b) Cloke, F. G. N.; Flower, K. R.; Hitchcock, P. B.; Nixon, J. F. *J. Chem. Soc., Chem. Commun.* **1995**, 1659−1660.

(7) Gradoz, P.; Baudry, D.; Ephritikhine, M.; Nief, F.; Mathey, F. *J. Chem. Soc., Dalton Trans.* **1992**, 3047−3051.

(8) Kostic, N. M.; Fenske, R. F. *Organometallics* **1983**, *2*, 1008−1013. Guimon, C.; Gonbeau, D.; Pfister-Guillouzo, G.; de Lauzon, G.; Mathey, F. *Chem. Phys. Lett.* **1984**, *104*, 560−567. Su, M.-D.; Chu, S.-Y. *J. Phys. Chem.* **1989**, *93*, 6043−6051.

(9) De Lauzon, G.; Deschamps, B.; Fischer, J.; Mathey, F.; Mitschler, A. *J. Am. Chem. Soc.* **1980**, *102*, 994−1000.

S0276-7333(97)00561-X CCC: $14.00

Table 1. NMR Signal Shifts of $(Tmp)_2Cr$ and $[(Tmp)_2Cr]^+[B(C_6H_5)_4]^-$

	nucleus						
shift[a]	P	C2/5	C3/4	Ca2/5	Ca3/4	Hβ2/5	Hβ3/4
				$(Tmp)_2Fe$[b]			
δ[c]	−58.5	94.0 (55.2)	95.1 (<1)	14.1 (24.4)	12.7 (<1)	1.65 (9.4)	1.83 (<0.5)
				$(Tmp)_2Cr$[d]			
δ^{exptl}	−173	28.8	−376	12.9	245	34.0	−39.4
δ^{para}	−115	−65.2	−471	−1.2	232	32.4	−41.2
δ^{dip} [e]	50.6	56.8	53.7	−2.7	−2.6	−6.9	−6.7
δ^{con}	−166	−122.0	−525	1.5	235	39.3	−34.5
				$[(Tmp)_2Cr]^+$[f]			
δ^{exptl}						43.1	24.3
δ^{para}						41.5	26.1

[a] In ppm. δ^{exptl}, δ^{para}, δ^{dip}, and δ^{con} are the experimental (relative to TMS), the paramagnetic, the dipolar, and the contact shift, respectively. [b] In C_6D_6 at 298 K. [c] Coupling to ^{31}P (Hz) in parentheses. [d] ^1H NMR in C_6D_6 at 298 K; ^{13}C and ^{31}P NMR at 413 and 368 K, respectively; solvent, anisole. [e] Calculated values (cf. Supporting Information). [f] In CD_3NO_2 at 298 K; resonances of $[B(C_6H_5)_4]^-$ at 7.34, 6.99, and 6.83 ppm (ratio 2/2/1).

Scheme 1[a]

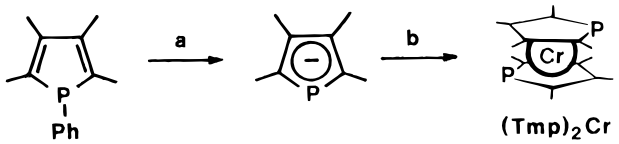

[a] Key (a) K, dimethoxyethane; (b) $CrCl_2(THF)$.

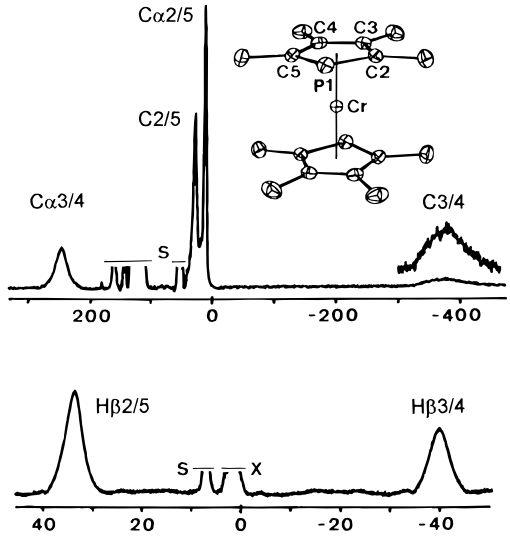

Figure 1. NMR spectra[11] and molecular structure of $(Tmp)_2Cr$. ^{13}C NMR spectrum (top) at 413 K; solvent anisole. ^1H NMR spectrum (bottom) at 298 K; solvent, C_6D_6. S and X are the solvent and impurities, respectively; scale in ppm. Selected distances (Å) and angles (deg): Cr−P1 2.3642(4), Cr−C2 2.170(1), Cr−C3 2.205(1), Cr−C4 2.207(1), Cr−C5 2.172(1), P1−C2 1.787(1), P1−C5 1.792(2), C2−C3 1.421(2), C3−C4 1.416(2), C4−C5 1.411(2); C2−P1−C5 89.05(7).

also found for the couple Cp_2Cr/Cp_2Fe and that follows from the electron count.[10]

The structure in solution was confirmed by the ^{13}C and ^1H NMR spectra (Figure 1), which showed the expected number of signals. In addition, a ^{31}P NMR signal was observed (Table 1). It is worth noting that the relaxation which is reflected by the signal width does not allow nuclear coupling with ^{31}P to be observed. The assignment of one of the ^{13}C NMR signals is based on the fact that the signal near 10 ppm is a quartet due to the one-bond C,H coupling of a CH_3 group. The only other signal whose width would allow C,H coupling to be observed is that near 30 ppm. Since no coupling was detected, this signal must be assigned to a ring-C rather than to the second methyl-C atom. Hence, in general, the signals of the ring-C and Cα[11] atoms are found at low and high frequency, respectively, relative to the reference signals of diamagnetic $(Tmp)_2Fe$ (cf. Table 1). This pattern has been previously observed for chromocenes[4,12] and is indicative of a negative spin density on the ligands.

Chart 1. Ligand π Orbitals Involved in Spin Delocalization

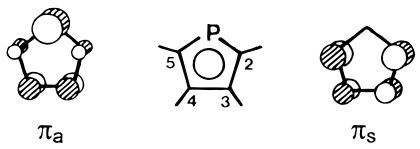

Further distinction of the nuclei in positions 2/5 and 3/4 of $(Tmp)_2Cr$ is of relevance because it is related to the spin density distribution within the Tmp ligands which we are interested in. As far as the ligand π orbitals are concerned, the spin may reside in the symmetric and antisymmetric (with respect to the C_2 axis) e_1-type MOs (molecular orbitals) π_s and π_a, respectively, which are shown in Chart 1. For chromocene, the π_s- and π_a-containing MOs are degenerate, while they are split for $(Tmp)_2Cr$ as a result of the perturbation introduced by the phosphorus atoms.[8] This means that for chromocene both π_s and π_a equally contribute to the spin delocalization, while for $(Tmp)_2Cr$ one of these MOs dominates, and this must be reflected in the NMR spectra. Actually, the squared coefficients of the $2p_z$ AOs (atomic orbitals) (qualitatively given in Chart 1 by different lobe diameters) are related to the hyperfine coupling constants $A(X)$ expected for the nucleus X,[13] and these are proportional to the NMR contact shifts δ^{con}. When this is combined with the negative overall spin on the Tmp ligand, the ^{31}P NMR signal of

(10) Haaland, A. *Acc. Chem. Res.* **1979**, *12*, 415−422.

(11) α and β designate nuclei which are separated from the ring by one and two bonds, respectively.

(12) (a) Köhler, F. H. *J. Organomet. Chem.* **1976**, *113*, 11−32. (b) Köhler, F. H.; Doll, K.-H.; Prössdorf, W. *J. Organomet. Chem.* **1982**, *224*, 341−353. (c) Köhler, F. H.; Doll, K.-H. *Z. Naturforsch. B: Chem. Sci.* **1982**, *37*, 144−150. (d) Köhler, F. H.; Geike, W. *J. Organomet. Chem.* **1987**, *328*, 35−47. (e) Blümel, J.; Hofmann, P.; Köhler, F. H. *Magn. Reson. Chem.* **1993**, *31*, 2−6. Note that inverted shift signs were used in a−d.

(13) Karplus, M.; Fraenkel, G. K. *J. Chem. Phys.* **1961**, *35*, 1312−1323. Yonezawa, T.; Kawamura, T.; Kato, H. *J. Chem. Phys.* **1969**, *50*, 3482−3492.

$(Tmp)_2Cr$ should have a negative shift if the π_a orbital dominates. In contrast, the shift should be positive if the π_s orbital dominates strongly. The large negative ^{31}P NMR signal shift favors the π_a orbital, and hence the signal of C3/4 must be shifted to a lower frequency than that of C2/5.

The ^{13}C NMR signal pattern is striking in that the splitting is much larger than that known for any substituted chromocene so far. Because the signal splitting increases with the separation of the π_a- and π_s-containing MOs, we conclude that the spin localization within the ligands of $(Tmp)_2Cr$, mainly at P and C3/4, is much more pronounced than for chromocenes.

As for the ^1H NMR, all of the protons of Tmp are β protons and, thus, their signal shift is strongly influenced by hyperconjugative spin transfer from the p_z orbitals of the neighboring ring-C atoms.[4] Given the negative spin at C2−C5, we therefore expect two signals at the low-frequency side. The signal of Hβ3/4 should be more shifted than that of Hβ2/5, again following the relative size of the coefficients of π_a in Chart 1. In contrast, Figure 1 shows one signal at either frequency side. In order to explain this observation, dipolar shifts, δ^{dip}, and σ delocalization must be taken into account.[4,12] Calculation of the dipolar shifts (Table 1) yields δ^{dip}(Hβ2/5) = −6.9 and δ^{dip}(Hβ3/4) = −6.7 at 298 K, which are too small to account for the experimental data. Rather, σ delocalization should be the reason. It shifts all signals to high frequency, and consequently, δ^{para}(Hβ2/5) becomes positive while δ^{para}(Hβ3/4) remains negative. The NMR data of other chromocenes clearly show that σ delocalization significantly contributes to the signal shifts.[14] Note that $(Me_4C_5H)_2Cr$,[12c] which is the CH analogue of $(Tmp)_2Cr$, has a very similar ^1H NMR spectrum, although the signal splitting is smaller (as expected from a smaller perturbation).

Once the signal assignment has been established, the experimental shifts can be converted to δ^{para} values by referencing to the corresponding signals of $(Tmp)_2Fe$. Finally $\delta^{para} - \delta^{dip}$ yields δ^{con}, and these data are collected in Table 1. It is gratifying that, in retrospect, the δ^{con} values confirm the reasoning which led to the π_a orbital (Chart 1) as being mainly responsible for the spin distribution within the ligands.

The concentration of spin at certain ligand nuclei can be verified independently by temperature-dependent NMR studies. Suppose that the MOs relevant for the spin distribution contain the ligand orbitals π_a and π_s, as mentioned (Chart 1), and that the energy separation between them is comparable to the thermal energy with the π_a-containing MO being more important than the other. On increasing the temperature, the population of the MOs is changed in such a way that the π_s contribution becomes more important. As a consequence, the spin should increase on C2/5 and decrease on C3/4 and the NMR signal shifts should no longer follow the Curie law which would require $\delta^{para} \propto T^{-1}$ or $\delta^{para}T/298 = \vartheta =$ constant (T is the absolute temperature and ϑ the reduced paramagnetic signal shift). This behavior has been observed previously.[16]

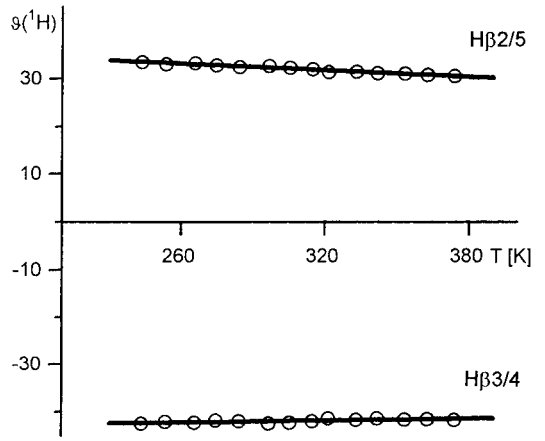

Figure 2. Temperature dependence of the ^1H NMR signal shifts of $(Tmp)_2Cr$ represented as a ϑ vs T plot (see text).

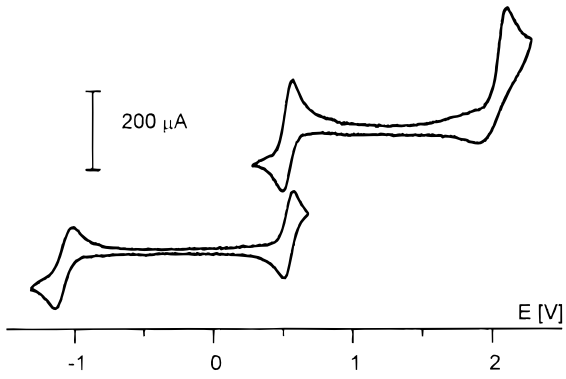

Figure 3. Cyclic voltammogram of $(Tmp)_2Cr$ (1.6×10^{-3} mol^{-1} in propionitrile, 25 °C). Supporting electrolyte, 0.1 M n-Bu_4NPF_6; scan rate, 200 m Vs^{-1}, scale relative to Cp_2Co/Cp_2Co^+.

With these facts in mind, the ^1H NMR spectra of $(Tmp)_2Cr$ were recorded between 243.5 and 374.0 K. The data was converted to ϑ values, as mentioned above, and plotted against T (Figure 2). In contrast to simple substituted chromocenes, ϑ for $(Tmp)_2Cr$ is essentially constant with T. This implies that only one of the π_a/π_s-containing MOs (i.e., π_a cf. above) determines the spin distribution within the ligand. This in turn confirms the strong perturbation which is introduced on going from Cp_2Cr to $(Tmp)_2Cr$.

In the cyclic voltammetry experiments at 25 °C, $(Tmp)_2Cr$ underwent a reversible oxidation at 0.56 V (ΔE_p = 70 mV) to the monocation, a quasi-reversible reduction at −1.07 V (ΔE_p = 95 mV) to the monoanion, and a second, irreversible oxidation at E_{p_a} = 2.23 V; here ΔE_p is the separation $E_{p_a} - E_{p_c}$ between the anodic and cathodic peak potential, respectively, and all potentials are relative to the potential of the internal couple Cp_2Co/Cp_2Co^+. The potential of the first two electron transfers was about 0.3 V higher than that for Cp_2Cr in the same solvent.[17] This must be ascribed to the

(14) For alkylated chromocenes, the ^{13}C NMR signal shifts of the ring-C atoms (C1−C5) are less shifted than those of the respective next-neighbor carbons of the substituent (Cα).[11a−c] The reason is that on C1−C5 the spin resulting from π and σ delocalization has opposite signs while it has the same sign at Cα. The same phenomenon was encountered previously for other paramagnetic sandwich compounds.[15]

(15) Hebendanz, N.; Köhler, F. H.; Müller, G.; Riede, J. *J. Am. Chem. Soc.* **1986**, *108*, 3281−3289. Köhler, F. H.; Metz, B.; Strauss, W. *Inorg. Chem.* **1995,** *34*, 4402−4413.

(16) Köhler, F. H.; Geike, W. *J. Magn. Reson.* **1983**, *53*, 297−302. Köhler, F. H.; Cao, R. D.; Manlik, G. *Inorg. Chim. Acta* **1984**, *91*, L1−L2. Note that the shift signs were changed since this publication.

(17) (a) Atzkern, H.; Bergerat, P.; Fritz, M.; Hiermeier, J.; Hudeczek, P.; Kahn, O.; Kanellakopulos, B.; Köhler, F. H.; Ruhs, M. *Chem. Ber.* **1994**, *127*, 277−286. (b) Lemoine, P.; Gross, M.; Braunstein, P.; Mathey, F.; Deschamps, B.; Nelson, J. H. *Organometallics* **1984**, *3*, 1303−1307.

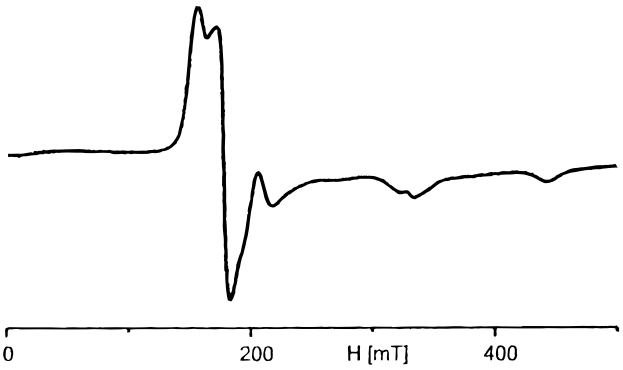

Figure 4. X-band EPR spectrum of $[(Tmp)_2Cr]^+[B(C_6H_5)_4]^-$ (powder at 135 K).

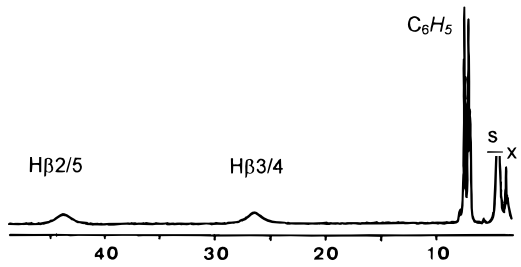

Figure 5. ^1H NMR spectrum of $[(Tmp)_2Cr]^+[B(C_6H_5)_4]^-$ in CD_3NO_2 at 303 K. S and X are the solvent and impurity, respectively; scale in ppm.

combined effect of the heteroatom and the methyl substituents.[17b]

Chemical oxidation with $[(MeC_5H_4)_2Fe]^+[B(C_6H_5)_4]^-$ gave $[(Tmp)_2Cr]^+[B(C_6H_5)_4]^-$ as an air-sensitive red powder in 65% yield. Because it is a Cr(III) sandwich complex it must have three unpaired electrons, and this is reflected in both the EPR and NMR spectra. $[(Tmp)_2Cr]^+$ salts are soluble in polar solvents, whereas they decompose readily when the solvent is a good donor. Therefore, the solid-solution EPR spectra showed varying amounts of impurities. A clean spectrum was obtained from $[(Tmp)_2Cr]^+[B(C_6H_5)_4]^-$ powder (Figure 4); the surprisingly good resolution might be due to the separation of the paramagnetic cations by the bulky anions. The features centered at 160, 180, 215, 330, and 530 mT are similar to what is expected for $S = {}^3/_2$ ions having an (almost) isotropic g factor and a zero-field splitting smaller than 5 cm^{-1}.[18]

The ^1H NMR spectrum (Figure 5) showed two methyl signals near 26 and 43 ppm and three phenyl resonances in the usual range (cf. Table 1). Thus, upon oxidation the mean paramagnetic signal shift changes the sign. This corresponds to passing, for instance, from $(EtMe_4C_5)_2Cr$ ($\delta(H\beta_{av}) = -9.1$[12b]) to $[EtMe_4C_5)_2Cr]^+$ ($\delta H\beta_{av} = 3.1$[4]), which both have negative spin density on their ligands. The reason for the change of signs may be an increase of the σ delocalization already mentioned, while the dipolar signal shifts should be small owing to the presumably small g-factor anisotropy.[19] Compared to $(Tmp)_2Cr$, the proton signal splitting of $[(Tmp)_2Cr]^+$ is smaller. This is a general feature of $S = {}^3/_2$ metallocenes and follows from the fact that spin density resides in both the π_a- and π_s-containing MOs. In such cases, the NMR signal shifts should follow the Curie law. This was confirmed by temperature-dependent proton NMR measurements. Figure 6 shows that the reduced paramagnetic signal shifts are almost constant, as expected. It follows that, unlike in $(Tmp)_2Cr$, the spin density must be distributed more evenly on the ligand atoms of $[(Tmp)_2Cr]^+$, including phosphorus. Both $(Tmp)_2Cr$ and its cation are, therefore, susceptible to transfering spin to neighboring molecules via the P donor.

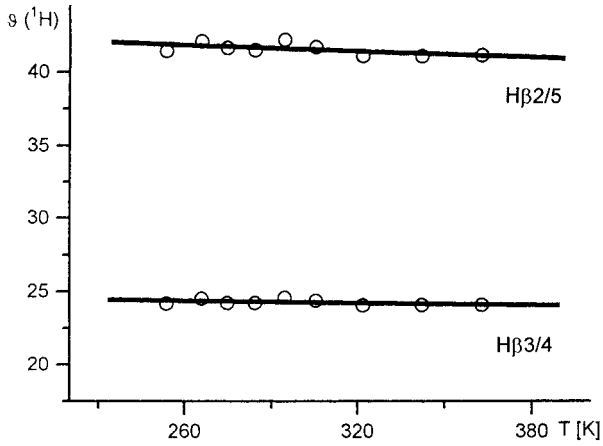

Figure 6. Temperature dependence of the ^1H NMR signal shifts of $[(Tmp)_2Cr]^+[B(C_6H_5)_4]^-$ represented as a ϑ vs T plot (see text).

Experimental Section

The synthetic work and the characterization were carried out under purified dinitrogen by using combined Schlenk/cannula techniques with dry, oxygen-free solvents. The mass spectrum was obtained with a Varian MAT 311 spectrometer. The EPR spectrum was measured with a Jeol JES RE 2X spectrometer working at 9.04 GHz; MnO diluted in MgO was used for calibration. The NMR spectra were run with Bruker MSL 300 and Jeol JNM GX 270 spectrometers. The equipment used for the cyclic voltammetry measurements has been described previously.[20] Traces of water were removed from the solution by passing it through a column with activated alumina integrated in the electrolysis cell, and $Cp_2Co^+PF_6^-$ was added as an internal standard. The elemental analyses were carried out in Inorganic Microanalytical Laboratory at Garching, Germany.

Bis(tetramethylphospholyl)chromium ($(Tmp)_2Cr$). A solution of 1.16 g (6.5 mmol) of Me_4C_4PK[7] in 80 mL of THF was prepared at 25 °C, and 0.59 g (3.0 mmol) of $CrCl_2(THF)$ was added. The mixture, which became dark red-brown immediately, was stirred overnight, the solvent was stripped, and the residue was extracted with diethyl ether. Filtration via cannula and prolonged cooling to −35 °C gave 0.8 g (80.7% relative to $CrCl_2(THF)$) of red crystals of $(Tmp)_2Cr$, mp 157−8 °C. MS (m/z): 330 (100, M^+), 315 (6, $M^+ - CH_3$), 190 (4, $M^+ - C_8H_{12}P$), 165 (4, M^{2+}). Anal. Calcd for $C_{16}H_{24}CrP_2$: C, 58.18; H, 7.32; Cr, 15.75; P, 18.75. Found: C, 58.02; H, 7.43; Cr, 15.62; P, 18.24.

Bis(tetramethylphospholyl)chromium Tetraphenylborate. ($[(Tmp)_2Cr]^+[B(C_6H_5)_4]^-$). A 1.43 g (2.7 mmol) amount of $[(CH_3C_5H_4)_2Fe]^+[B(C_6H_5)_4]^-$ was added quickly to a stirred solution of 0.89 g (2.7 mmol) of $(Tmp)_2Cr$ in 50 mL of THF. The blue solid ferrocenium salt disappeared within 1 h while a red precipitate was formed. The solvent was removed via cannula, and the solid was washed with 50 mL portions of hexane until the solution was colorless. After drying in vacuo,

(18) Collison, D.; Mabbs, F. E. *J. Chem. Soc., Dalton Trans.* **1982**, 1565−1574.

(19) Kurland, R. J.; McGarvey, B. R. *J. Magn. Reson.* **1970**, *2*, 286−301.

(20) Atzkern, H.; Hiermeier, J.; Köhler, F. H.; Steck, A. *J. Organomet. Chem.* **1991,** *408*, 281.

Table 2. Crystal Structure Data

formula; mol wt	$C_{16}H_{24}CrP_2$; 330.31
cryst description	orange plate; 0.35 × 0.35 × 0.25 mm
cryst syst	monoclinic
space group	$P2_1/n$ (No. 14)
cell constants	$a = 7.800(1)$ Å, $b = 12.514(1)$ Å
	$c = 8.821(1)$ Å, $\beta = 109.34(1)°$
	$V = 812.41(3)$ Å^3, $Z = 2$
	$d_{calcd} = 1.350$ g cm^{-3}
diffractometer	Enraf-Nonius CAD4
corrections	Lorentz−polarization
temp	-150 ± 0.5 °C
radiation	Mo Kα ($\lambda = 0.710\ 73$ Å), graphite monochromator
abs coeff	$\mu = 8.7$ cm^{-1}
$F(000)$	348
θ range	$2° \le 2\theta \le 60.0°$
hkl ranges	$h = 0-10$, $k = 0-17$, $l = -12$ to 11
no. of reflns collected	2629 total, 2361 unique
no. of reflns included	2094 with $F_o^2 > 3.0\sigma(F_o^2)$
no. of params refined	88
goodness of fit	1.37
R, R_w	0.028, 0.061
minimization function	$(\|F_o\| - \|F_c\|)^2$, where $w = 4F^2/\sigma^2(F^2)$
least-squares function	$4F_o^2/\sigma^2(F_o^2)$, with $\sigma^2(F^2) = \sigma^2(I) + (pF^2)^2$

$[(Tmp)_2Cr]^+[B(C_6H_5)_4]^-$ was obtained as a dark red microcrystalline powder (yield 1.15 g, 65%). Anal. Calcd for $C_{40}H_{44}BCrP_2$: C, 73.96; H, 6.83; Cr, 8.01; P, 9.54. Found: C, 73,21; H, 6.91; Cr, 7.81; P, 9.67.

X-ray Structure Determination. Crystals of $(Tmp)_2Cr$ were grown from a diethyl ether solution of the compound by cooling. The crystallographic details are collected in Table 2. The structure was solved and refined by using the Enraf-Nonius MOLEN package. The molecule occupies a crystallographic symmetry center. The Cr and P atoms were located from a Patterson map; all other atoms were obtained from a standard Fourier synthesis. The hydrogens are occupying the two possible conformations and were included as fixed contributions in the final stages of the least-squares refinement while using anisotropic temperature factors for all other atoms. A non-Poisson weighting scheme was applied with a p factor of 0.08.

Acknowledgment. Support from the Fonds der Chemischen Industrie (Frankfurt), the Ecole Polytechnique, and the CNRS is gratefully acknowledged.

Supporting Information Available: Text giving the details of the calculation of the dipolar shifts, tables containing positional parameters, bond lengths, bond angles, and least-squares planes, and an ORTEP diagram (8 pages). Ordering information is given on any current masthead page.

OM9705618